

CHALMERS



UNIVERSITY OF GOTHENBURG

PREPRINT 2013:8

A spatial-temporal model for wind speeds variability

IGOR RYCHLIK
AMIR MUSTEDANAGIC

Department of Mathematical Sciences

Division of Mathematical Statistics

CHALMERS UNIVERSITY OF TECHNOLOGY

UNIVERSITY OF GOTHENBURG

Gothenburg Sweden 2013

Preprint 2013:8

**A spatial-temporal model for wind speeds
variability**

Igor Rychlik and Amir Mustedanagic

Department of Mathematical Sciences
Division of Mathematical Statistics
Chalmers University of Technology and University of Gothenburg
SE-412 96 Gothenburg, Sweden
Gothenburg, June 2013

Preprint 2013:8
ISSN 1652-9715

Matematiska vetenskaper
Göteborg 2013

A spatial-temporal model for wind speeds variability

IGOR RYCHLIK AND AMIR MUSTEDANAGIC

Mathematical Sciences,
Chalmers University of Technology,
SE-412 96 Göteborg, Sweden.

Abstract

Wind speeds are modeled by means of a spatial-temporal transformed Gaussian field. Its dependence structure is localized by introduction of time and space dependent parameters in the spectrum. The model has the advantage of having a relatively small number of parameters. These parameters have natural physical interpretation and are statistically fitted to represent variability of observed wind speeds in ERA Interim reanalysis data set.

Keywords: Wind speeds, wind-energy, spatio-temporal model, Gaussian fields.

1 Introduction

In the literature typically distribution of wind speed is understood as the long-term distribution of the wind speeds at some location or region. The distribution can be interpreted as variability of W at a randomly taken time during a year. The Weibull distribution gives often a good fit. Limiting time span to, for example, January month affects the W distribution simply because, as it is the case for many geophysical quantities, the variability of W depends on season. To avoid ambiguity when discussing the distribution of W , time span and region over which the observations of W are gathered need to be clearly specify. By shrinking the time span to a single moment t and geographical region to a location \mathbf{p} one obtains (in the limit) the distribution of $W(\mathbf{p}, t)$ and this will be the meaning of distribution of W as used in this paper. Obviously the long-term distribution can be retrieved from the "local" $W(\mathbf{p}, t)$ distributions by means of an average of the local distributions over a year. In this paper a new stochastic model for the wind speed variability in time and over a large geographical region is proposed.

In order to identify the distributions at all positions \mathbf{p} and times t vast amount of data are needed. Here we shall utilize reconstruction of W from numerical ocean-atmosphere models based on large-scale meteorological data, called also reanalysis, to fit a model. While a reanalysis does not represent actual measurements of quantities but extrapolations to the grid locations based on simulations from complex dynamical models, it is defined on regular grids in time and space and hence convenient to use. Here the model has been fitted to ERA Interim data

<http://www.ecmwf.int/products/data/archive/descriptions/ei/index.html>

produced by European Centre for Medium-Range Weather Forecasts. However the model can also be fitted to other data sets, e.g. to satellites wind measurements which has also good spatial coverage, see [3].

The paper is organized as follows. In the next section a general construction of non-stationary model for wind speed variability in time and space is presented. In Section 3 an parametric covariance function describing time space correlations of wind speed field is introduced and means to estimate the model presented. The physical interpretations of the introduced parameters are also discussed in this section. In Section 4 in situ measured wind speeds are used for validation of the model. Long term distributions of wind speeds and persistence statistics are used for the validation. The paper closes with conclusions and list of references.

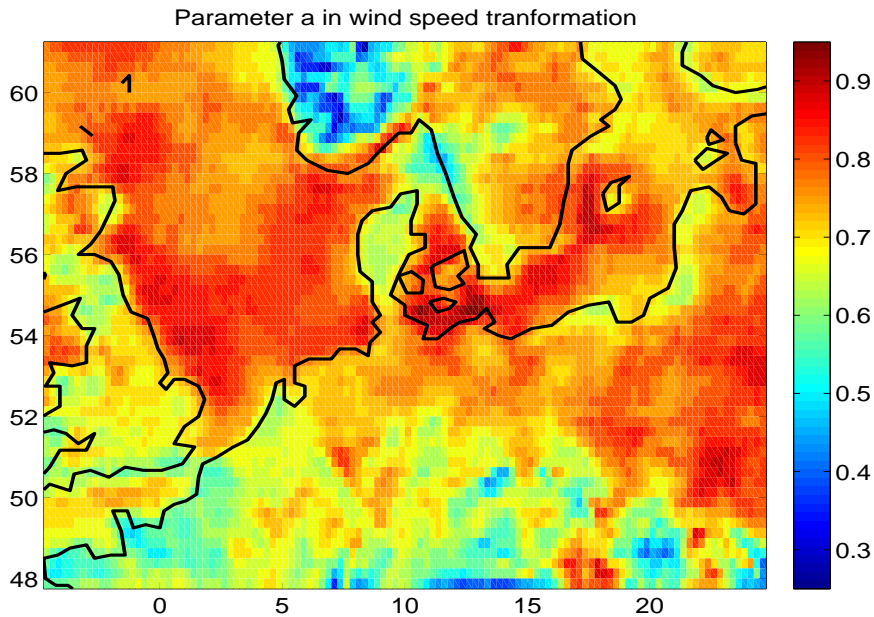


Figure 1: Values of parameter a in the transformation (1)

2 Gaussian model for transformed wind field

In order to make notation more compact we will not always distinguish between space and time coordinates and equivalently use notations \mathbf{x} or (\mathbf{p}, t) for (x, y, t) . Note that units of t are hours, with $t = 0$ at 1 January.

In this paper the field $W(\mathbf{x})$ will be transformed in order to improve accuracy of Gaussian distribution fit to wind field data, viz.

$$W(\mathbf{x})^a = m(\mathbf{x}) + X(\mathbf{x}), \quad 0 < a \leq 1, \quad (1)$$

where X is zero mean Gaussian field. The transformation is often used to describe variability of wind speeds in time at fixed location, see eg. [6]. In Figure 1 estimates of parameter a are presented. At offshore locations the parameter values vary around 0.8 while for close to shore or inlands locations a is often smaller. Note that smaller values of a indicate larger departures of the observed wind speeds distribution from the Gaussian one.

By assuming that $X(\mathbf{x})$ is a zero mean Gaussian field, the model for wind speeds $W(\mathbf{x})$ is completely specified if additionally to the expected value $m(\mathbf{x})$, variance $\sigma^2(\mathbf{x})$ the autocorrelation function $\rho(\mathbf{x}, \mathbf{x}')$ is given. The parameters $m(\mathbf{x})$ and $\sigma^2(\mathbf{x})$ will be estimated by means of regression on a seasonal component. The results can be presented as maps, see Figures 2-3, where top plots present medians of wind speeds in February and August, respectively. The corresponding 10% quantiles are given in bottom plots. As expected the typical seasonal and geographical variability of wind speeds can be observed, e.g. winds are stronger offshore than inlands and in winter than in summer. Finding a suitable model for $\rho(\mathbf{x}, \mathbf{x}')$ is a more delicate issue, see e.g. [10] for survey of different models. Here we will follow the method used for modeling correlations between significant wave height proposed in [3] see also [7] while in [8] some related covariance models are presented.

The model for correlation $\rho(\mathbf{x}, \mathbf{x}')$ is constructed in two steps. First one is assuming that locally, e.g. in a geographical region of four by four degree and time span of a week, the wind speed field can be accurately modeled by means of a stationary field. The local models are then used to evaluate a global model in a larger scale, see [5] for mathematical details. Here we present only the resulted formula for the covariance

$$\mathbb{C}(\mathbf{x}, \mathbf{x}') = \rho(\mathbf{x}, \mathbf{x}')\sigma(\mathbf{x})\sigma(\mathbf{x}').$$

As mentioned above the construction consists of two steps given next;

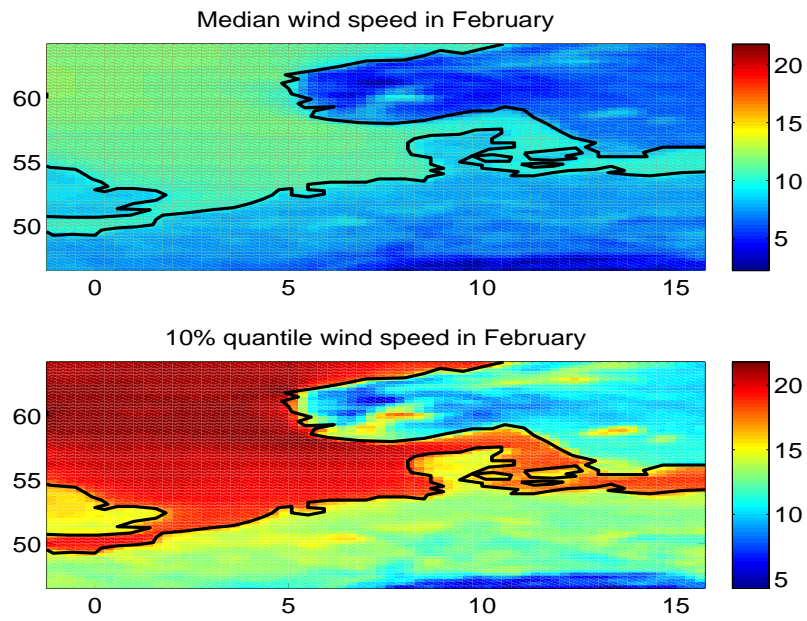


Figure 2: Estimates of the median wind speed in February top plot. Estimates of the 10% quantile of the wind speed in February bottom plot.

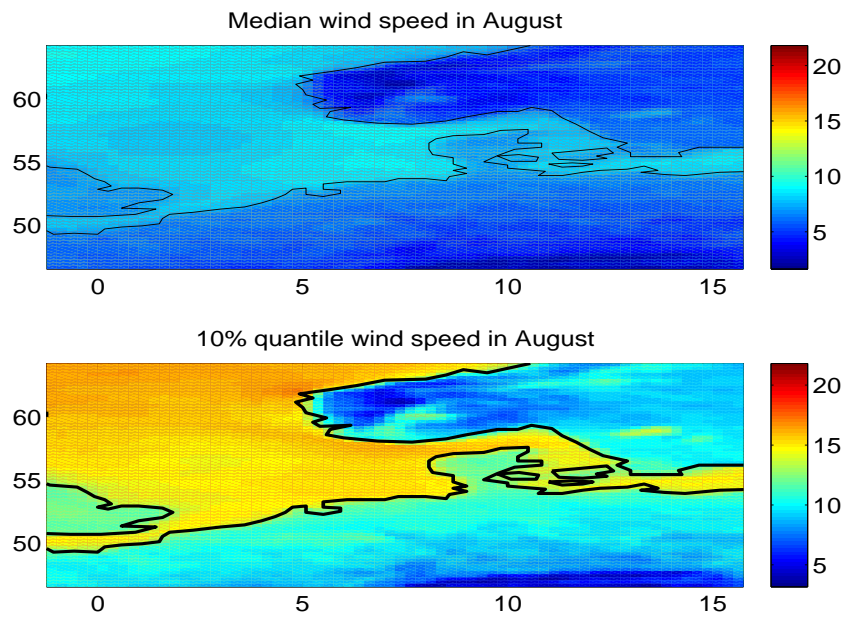


Figure 3: Estimates of the median wind speed in August top plot. Estimates of the 10% quantile of the wind speed in August bottom plot.

Step 1: Consider first a position $\mathbf{x}_0 = (\mathbf{p}_0, t_0)$. The residual wind speed field $X(\mathbf{x})$, defined in (1), limited to a neighborhood of the position $\mathbf{x}_0 = (\mathbf{p}_0, t_0)$, is modeled as a part of a homogeneous and stationary Gaussian field. The stationary field has a power spectral density (psd) $S(\kappa_x, \kappa_y, \omega)$. Since the psd often depends on \mathbf{x}_0 we shall include this dependence into notation and write $S_{\mathbf{x}_0}$ for the psd. The covariance function for local model of the field is then given by

$$\mathbb{C}_{\mathbf{x}_0}(\mathbf{x}, \mathbf{x}') = \int \exp(-i(\mathbf{x} - \mathbf{x}') \Omega) S_{\mathbf{x}_0}(\Omega) d\Omega, \quad (2)$$

where $\Omega = (\kappa_x, \kappa_y, \omega)$.

Step 2: Following approach presented in [5] the global model will have the covariance

$$\mathbb{C}(\mathbf{x}, \mathbf{x}') = \int \exp(-i(\mathbf{x} - \mathbf{x}') \Omega) \sqrt{S_{\mathbf{x}}(\Omega) S_{\mathbf{x}'}(\Omega)} d\omega. \quad (3)$$

Variability of the average wind speeds changes in different scales; months, days and hours. The seasonal variability is averaged and modeled by means of time variable parameters; means, variances and gradients covariances. The variability between days and hours is modeled by splitting the residual field X into two components; "slow" X^{sl} and "fast" X^f ($X(\mathbf{x}) = X^{sl}(\mathbf{x}) + X^f(\mathbf{x})$). We assume that the fields X^{sl} , X^f are independent and have covariance functions given by (5). For the slow component the parameters σ^2 , Λ are estimated using filtered wind speeds having harmonics with periods below five days removed. The parameters in fast components are estimated in the residual obtained by removing slow component from the wind speed data. In order to make formulas more transparent, in the following text, most often we will not distinguish between the fast and slow component.

3 The covariance model for residual wind speed field X

In this section we introduce a very simple model for the local psd $S_{\mathbf{x}_0}$

$$S_{\mathbf{x}_0}(\kappa_x, \kappa_y, \omega) = \sigma_{\mathbf{x}_0}^5 (2\pi)^{3/2} |\Lambda_{\mathbf{x}_0}|^{-1/2} e^{-\frac{\sigma_{\mathbf{x}_0}^2}{2} (\kappa_x, \kappa_y, \omega) \Lambda_{\mathbf{x}_0}^{-1} (\kappa_x, \kappa_y, \omega)^T}, \quad (4)$$

where $|A|$ denotes determinant of a matrix A . Note that the psd $S_{\mathbf{x}_0}$ depends on location $\mathbf{x}_0 = (\mathbf{p}_0, t_0)$ through variance $\sigma_{\mathbf{x}_0}^2$ and the matrix $\Lambda_{\mathbf{x}_0}$.

Important advantage of the local model (4) is that the global covariance (3) can also be given by an explicit formula, viz.

$$\mathbb{C}(\mathbf{x}, \mathbf{x}') = \sigma_{\mathbf{x}} \sigma_{\mathbf{x}'} \sqrt{\frac{2^3 \sigma_{\mathbf{x}}^3 |\Lambda_{\mathbf{x}}|^{-1/2} \sigma_{\mathbf{x}'}^3 |\Lambda_{\mathbf{x}'}|^{-1/2}}{|\sigma_{\mathbf{x}}^2 \Lambda_{\mathbf{x}}^{-1} + \sigma_{\mathbf{x}'}^2 \Lambda_{\mathbf{x}'}^{-1}|}} e^{-\mathbf{z} (\sigma_{\mathbf{x}}^2 \Lambda_{\mathbf{x}}^{-1} + \sigma_{\mathbf{x}'}^2 \Lambda_{\mathbf{x}'}^{-1})^{-1} \mathbf{z}^T}, \quad (5)$$

where $\mathbf{z} = \mathbf{x}' - \mathbf{x} = (x' - x, y' - y, t' - t)$.

3.1 Estimation of parameter $\sigma_{\mathbf{x}_0}^2$ and the matrix $\Lambda_{\mathbf{x}_0}$ in (4)

Suppose that in a neighborhood of \mathbf{x}_0 the residual wind speed field X is homogeneous and posses a psd $S(\kappa_x, \kappa_y, \omega)$, in general not equal to (4). For the psd S the spectral moments are defined by

$$\lambda_{ijk} = \int \kappa_x^i \kappa_y^j \omega^k S(\kappa_x, \kappa_y, \omega) d\kappa_x d\kappa_y d\omega.$$

The spectral moments have the following interpretation

$$\lambda_{000} = \mathbb{V}(X(\mathbf{x}_0)), \quad \lambda_{200} = \mathbb{V}(X_x(\mathbf{x}_0)), \quad \lambda_{020} = \mathbb{V}(X_y(\mathbf{x}_0)), \quad \lambda_{002} = \mathbb{V}(X_t(\mathbf{x}_0)), \quad (6)$$

while

$$\lambda_{110} = \mathbb{C}ov(X_x(\mathbf{x}_0), X_y(\mathbf{x}_0)), \lambda_{101} = \mathbb{C}ov(X_x(\mathbf{x}_0), X_t(\mathbf{x}_0)), \lambda_{011} = \mathbb{C}ov(X_y(\mathbf{x}_0), X_t(\mathbf{x}_0)). \quad (7)$$

Next we compute the spectral moments λ_{ijk} for the psd $S_{\mathbf{x}_0}$. Simple calculus gives that $\sigma_{\mathbf{x}_0}^2 = \lambda_{000}$ while the $\Lambda_{\mathbf{x}_0}$ matrix is equal to

$$\Lambda_{\mathbf{x}_0} = \begin{pmatrix} \lambda_{200} & \lambda_{110} & \lambda_{101} \\ \lambda_{110} & \lambda_{020} & \lambda_{011} \\ \lambda_{101} & \lambda_{011} & \lambda_{002} \end{pmatrix}. \quad (8)$$

Consequently relations (6 - 8) give means to estimate the parameters in $S_{\mathbf{x}_0}$, defined in (4). More precisely $\sigma_{\mathbf{x}_0}^2$ can be estimated by the variance $\mathbb{V}(X(\mathbf{x}_0))$ while matrix $\Lambda_{\mathbf{x}_0}$ by the covariance matrix of the gradient vector $(X_x(\mathbf{x}_0), X_y(\mathbf{x}_0), X_t(\mathbf{x}_0))$.

The true psd S may differ considerably from the model $S_{\mathbf{x}_0}$. However the way parameters in $S_{\mathbf{x}_0}$ are fitted results in well calibrated model which preserves some important statistics. For example; the probability density of W ; the probability that maximum of residual wind speed in some surrounding of \mathbf{x}_0 exceeds a high level u , see [1] and [2] and the persistence statistics, see [11]. In the following subsection we present some physical quantities that can be derived from the matrix $\Lambda_{\mathbf{x}_0}$. The quantities could be used to propose a crude model for wind speeds variability using alternative means, e.g. subjective expert judgments or meteorological predictions of future climate.

3.2 Physical interpretation of the model parameters

In this section we fix location $\mathbf{x}_0 = (\mathbf{p}_0, t_0)$ and write Λ, σ^2 for $\Lambda_{\mathbf{x}_0}, \sigma_{\mathbf{x}_0}^2$, respectively. A "windy" region is defined as locations \mathbf{x} where wind speed W exceeds its median. The size of the region will be quantified using the residual field X defined in (1). From the definition of the wind speed field W (1) it directly follows that the windy region consists of locations \mathbf{x} where $X(\mathbf{x}) > 0$. In the next subsections we give some simple characteristics of the region assuming that X has psd (4)

3.2.1 Size of "windy" region

A simple measure of geometrical properties of the windy region are average lengths of excursions above zero by $X(\mathbf{x})$ along the x, y axis. Here the parameters will be called average lengths L_x, L_y and will be evaluated by means of Rice's formula [12], viz.

$$L_x = \pi \sqrt{\frac{\sigma^2}{\lambda_{200}}}, \quad L_y = \pi \sqrt{\frac{\sigma^2}{\lambda_{020}}}, \quad (9)$$

see [11] for details of derivations.

Estimates of the longitudinal size L_x of windy region for the fast component X^f in February and August are shown in Figure 4; top, bottom plots, respectively. The latitudinal size L_y for the fast component of wind speeds in February and August are shown in Figure 5; top, bottom plots, respectively.

3.2.2 Average duration of windy weather - Temporal model for wind speed

Similarly as the average sizes L_x, L_y , defined in (9), one can also introduce the average duration of windy region τ , say. Consider a fixed position \mathbf{x}_0 and denote by $X(t) = X(\mathbf{x}_0, t)$. For a short period of time, e.g. a week, $X(t)$ can be considered as a zero mean stationary Gaussian process. Then again using Rice's formula the average period X stays above zero is given by

$$\tau = \pi \sqrt{\frac{\sigma^2}{\lambda_{002}}}. \quad (10)$$

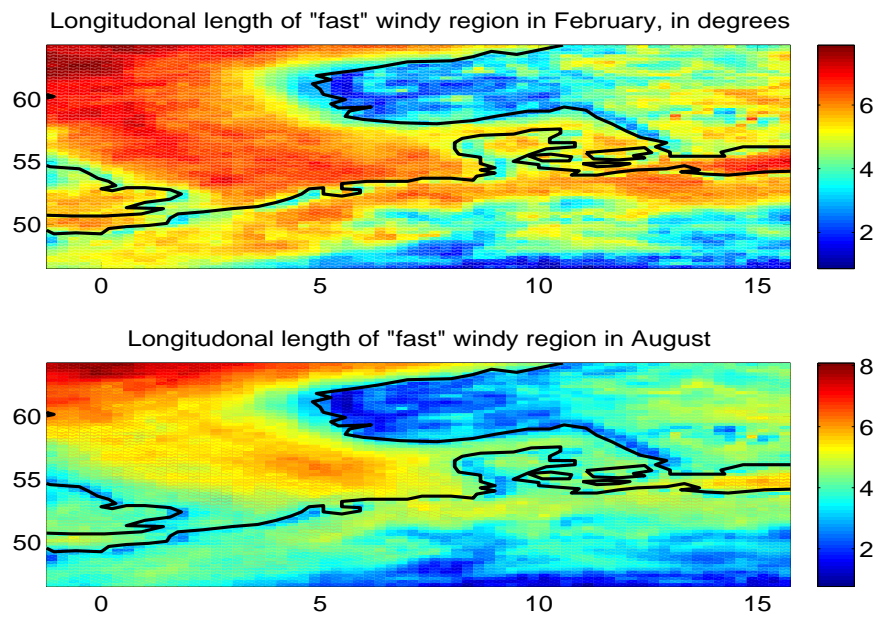


Figure 4: Estimates of the average length, in degrees, of windy region in longitude direction (x) for a fast component of wind speed field; (top) in February; (bottom) in August.

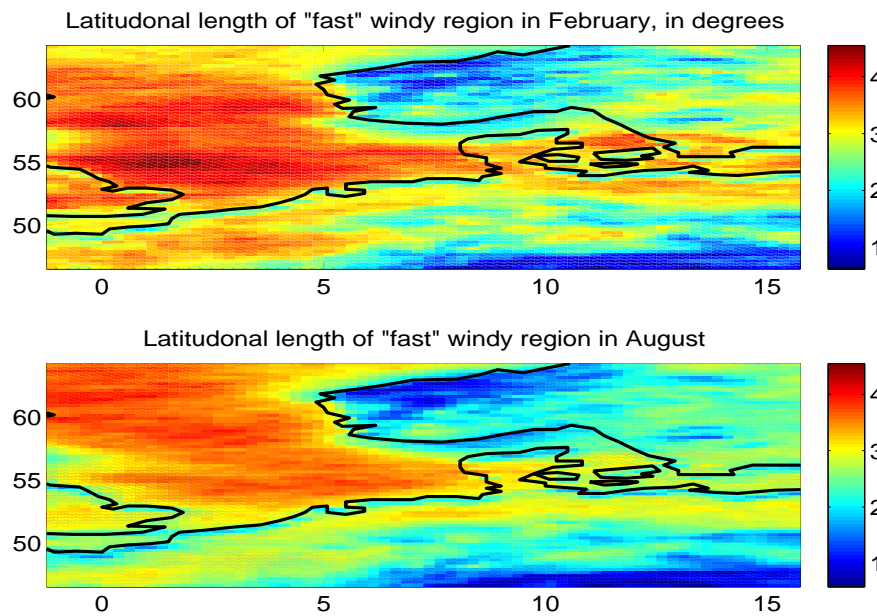


Figure 5: Estimates of the average length, in degrees, of windy region in latitude direction (y) for a fast component of wind speed field; (top) in February; (bottom) in August.

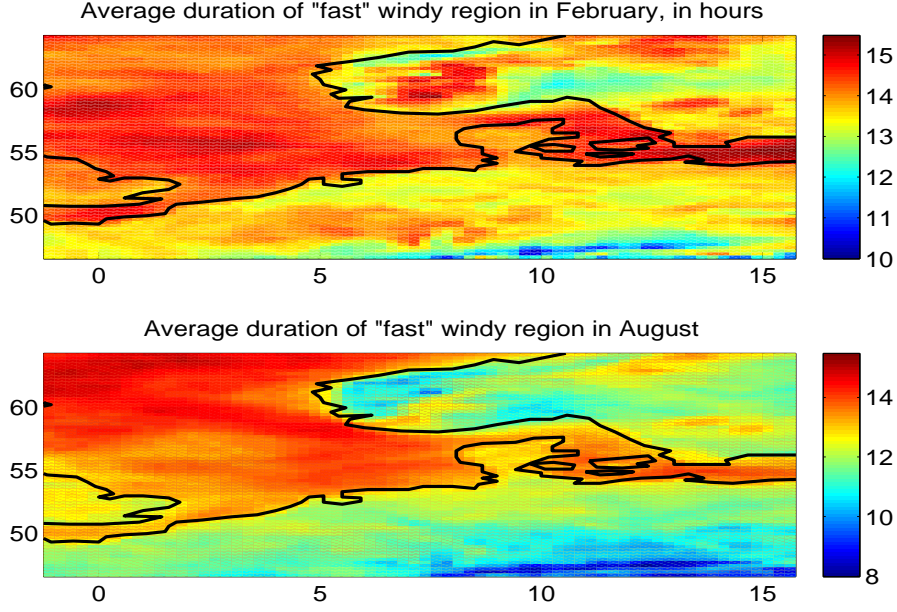


Figure 6: Estimates of time duration, in hours, of windy weather for a fast component of residual wind speed field X ; (top) in February; (bottom) in August.

This is an important parameter that together with variance σ^2 defines the temporal covariance function of $X(t)$, viz. (5)

$$\mathbb{C}(t, s) = \sigma^2 e^{-\pi^2(t-s)^2/(2\tau^2)}. \quad (11)$$

Note that τ , t and s should have the same units, here hours.

The average duration of windy weather, i.e. parameter τ , for the fast component is shown in Figure 6. One can see that the duration is approximately between 8 and 14 hours in average. In Figure 7 the duration of windy weather of slow component is shown in February top plot, and in August bottom plot. Now the durations are between 4 and 5 days which is not surprising since the slow component was defined by removing harmonics with periods shorter than 5 days from wind residual X .

3.2.3 Dynamics of "windy" regions

Another important parameters are velocities of "windy regions" movements. In pioneering work [9] a concept of velocity was introduced for random, moving surfaces. This concept of velocity has been further investigated in [4] to describe dynamics of contour levels in a moving random field. The zero-level contour of X field is the edge of a windy region and the velocities defined on that contour line $X(\mathbf{x}) = 0$ describe movements of the region of above median wind speeds. Note that the velocities of windy regions are not wind velocities itself.

Here the following definition for the velocity of movement of the residual field $X(\mathbf{x})$ at position \mathbf{x}_0 will be used

$$\mathbf{V}(\mathbf{x}) = \left(-\frac{X_t}{X_x}, -\frac{X_t}{X_y} \right).$$

The expected value of this velocity on the contour is given by

$$\mathbf{v} = (v_x, v_y) = \left(-\frac{\text{Cov}(X_t, X_x)}{\text{Var}(X_x)}, -\frac{\text{Cov}(X_t, X_y)}{\text{Var}(X_y)} \right) = \left(-\frac{\lambda_{101}}{\lambda_{200}}, -\frac{\lambda_{011}}{\lambda_{020}} \right). \quad (12)$$

In Figure 8 the average velocities v_x and v_y , for fast component, dependence on a location in February is shown while in Figure 9 the velocities, for the component, in August are given. As expected one can see that in average the windy regions moves from west to east over the seas. The velocities of windy regions of slow components are not shown since average movements of slow component are close to zero.

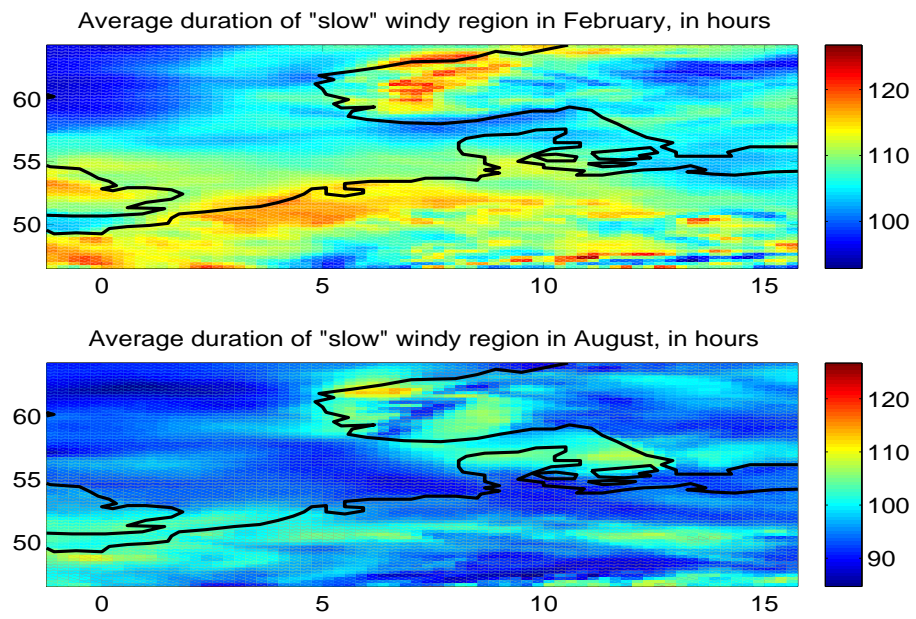


Figure 7: Estimates of time duration, in hours, of windy weather for a slow component of wind speed field X ; (top) in February; (bottom) in August.

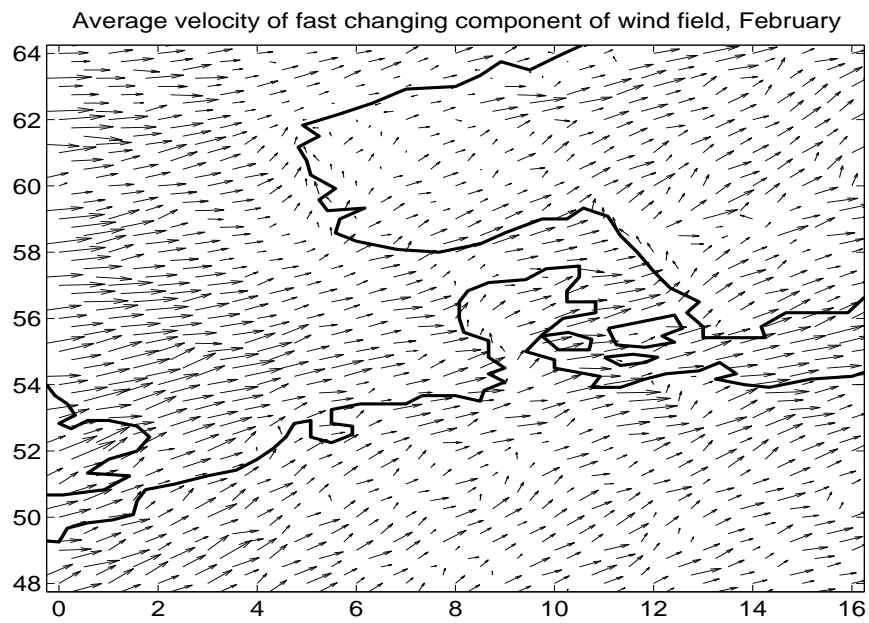


Figure 8: Estimates of the average velocities, [degrees/hour], windy regions of the fast component move in February.

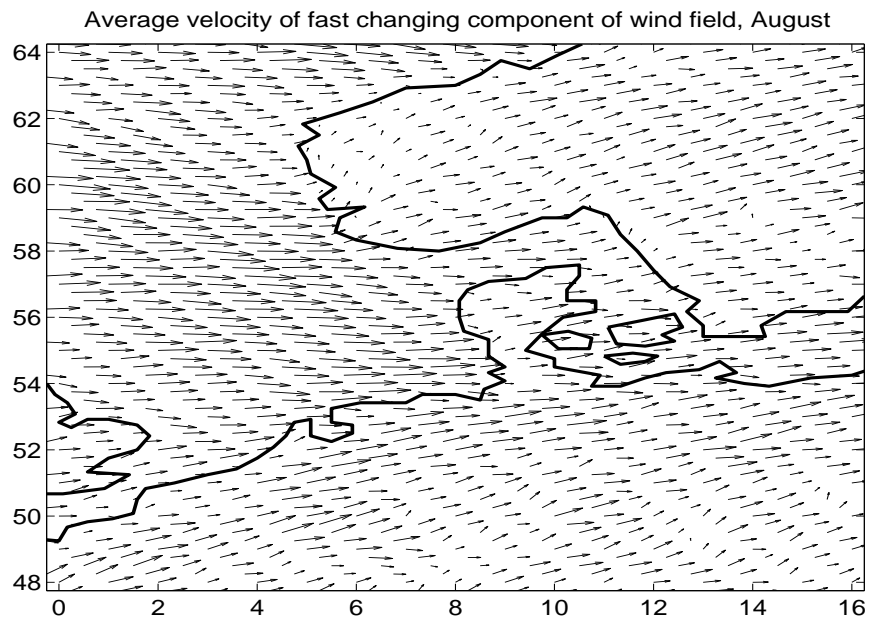


Figure 9: Estimates of the average velocities, [degrees/hour], windy regions of the fast component move in August.

Example: Simulation of wind field around Denmark

In Figure 10 simulation of wind speeds in February around Denmark are presented. The time difference between top and bottom simulation is three hours. This is relatively short period of time but changes in wind fields are clearly visible.

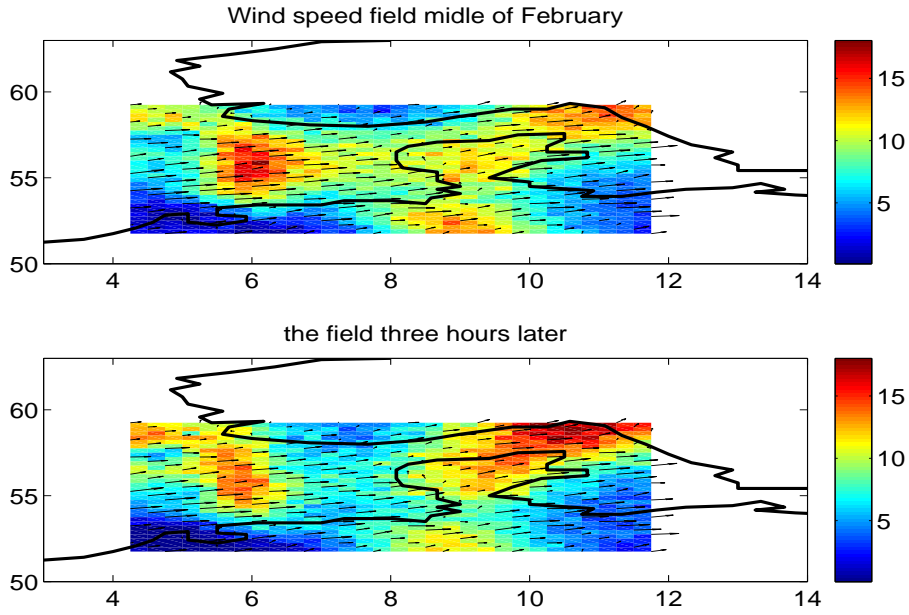


Figure 10: Simulation of wind speed field in February (top). The field three hours later (bottom). Arrows are the average velocities windy region movements.

4 Validation using measurements of wind speeds at Älvsborgsbron

In this section we use in situ wind measurements on Älvsborgsbron, from years 2005, 2006 and 2008, available at

<http://www.gvc2.gu.se/TAK-DATA/klimat.htm>

for validation of the proposed model. The bridge is located at 57,6967 N and 11,9869 E. Average wind speeds are recorded hourly. ERA Interim reanalysis at position 57.75 N and 12 E will also be employed. The validation will consist of two comparisons;

Firstly the yearly wind speed distributions for the in situ data and the reanalysis data at the position will be estimated. These empirical distributions will be compared with the theoretical distribution derived from the model.

Secondly, the persistence statistics of wind speeds will be found in the data sets and compared with average persistence computed from the model.

4.1 Temporal model for wind speeds at position 57.75 N and 12 E

ERA Interim data for 2007, 2008 and 2009 was used to estimate the spatio-temporal model, see e.g. Figures 4-8 for illustration of general variability of the parameters. Here we are limiting ourselves to one fixed location for which the parameter a in the transformation (1) is equal to 0.6. The mean value $m(t)$ is approximated by an seasonal component given by

$$m(t) = 3.06 + 0.275 \cos(2\pi\omega_y t) - 0.117 \sin(2\pi\omega_y t), \quad (13)$$

here t has units hours and $\omega_y = 1.141 \cdot 10^{-4}$. At this site the variances of the fast and slow components $X^f(t)$, $X^{sl}(t)$ seem to be constant and the estimated values of σ_f^2 , σ_{sl}^2 are 0.327, 0.489, respectively. Consequently the long-term distribution of wind speed at the location is given by

$$\mathbb{P}(W > w) = \int_0^{year} \Phi \left(\frac{m(t) - w^{0.6}}{\sqrt{\sigma_f^2 + \sigma_{sl}^2}} \right) dt, \quad (14)$$

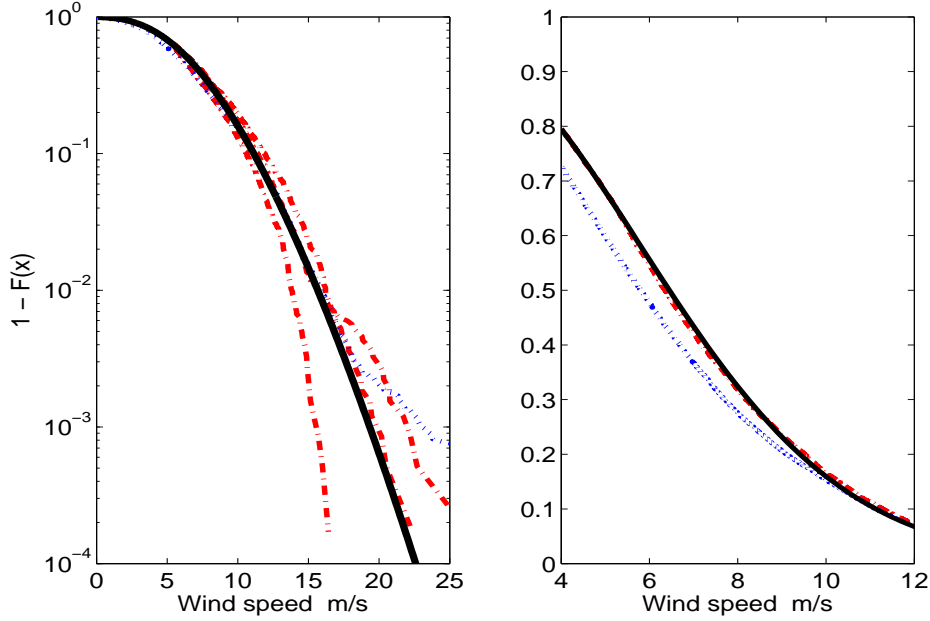


Figure 11: Long-term distribution of wind speeds $\mathbb{P}(W > w)$. Solid lines are the theoretical distribution computed from the model using (14) with parameters given in Section 4.1. Dashed dotted lines are $\mathbb{P}(W > w)$ estimated using ERA Interim for years 2007, 2008 and 2009. Dotted lines are estimates of $\mathbb{P}(W > w)$ for the in situ measured wind speeds for years 2005, 2006 and 2008. Left - logarithms of the probabilities highlighting the tails of the distributions; Right - zoomed left plot at the central part of the distributions.

where $\Phi(x)$ is the probability distribution of a standard Gaussian variable.

In Figure 11 the long-term $\mathbb{P}(W > w)$ estimated for ERA Interim data and the measured wind speeds are compared with the theoretical distribution computed by means of (14), presented as the solid lines. The dashed dotted lines are estimates of $\mathbb{P}(W > w)$ for ERA Interim, years 2007, 2008 and 2009. There are three dashed dotted lines representing estimates of the probabilities for the three years separately. We can see that just one year data may not be enough to accurately approximate $\mathbb{P}(W > w)$ for $w > 15$ m/s. (Note that in the right plot there is only one dashed dotted line. This is because in this plot the probability $\mathbb{P}(W > w)$ is estimated using all three years of ERA Interim data.)

The dotted lines are estimates of the probabilities for the in situ measured wind speeds at Älvsborgsbron years 2005, 2006 and 2008. One can see that distributions agrees very well with the theoretical one for high wind speeds. The probabilities of occurrences of moderate speeds are overestimated by both the model and the estimate derived from ERA Interim.

4.2 Persistence statistics

Persistence refers to the time for which a storm of a given severity or a period of calm is likely to persist. The simplest persistence statistics is the average persistence which is the expected period wind speed exceeds a fixed level w and can be computed as follows

$$T = t_{year} \mathbb{P}(W > w) / \mu(w), \quad (15)$$

where $\mu(w)$ is the expected number of times winds speed exceeds the threshold w during one year, \mathbb{P} is the long-term probability of wind speeds while $t_{year} = 24 \cdot 365.2$ is the number of hours during one year. The formula (15) follows from the fact that $t_{year} \mathbb{P}(W > w)$ is equal to the expected number of hours the wind speed is greater than w during one year.

For the proposed model $\mathbb{P}(W > w)$ is given by (14) while $\mu(w)$ can be estimated by means of

Rice's formula [12], see also [11], viz.

$$\mu(w) \approx \int_0^{year} \frac{1}{2\pi} \sqrt{\frac{\lambda_{002}(t)}{\lambda_{000}(t)}} e^{-\frac{(u^a - m(t))^2}{2\lambda_{000}(t)}} dt = \int_0^{year} \mu(w; t) dt, \quad (16)$$

where $\mu(w; t)$ is the intensity of level w upcrossings by the wind speed at time t . The formula is an approximation employing the following simplifying assumptions that $X(t)$ and $X'(t)$ are uncorrelated and that $m'(t) = 0$. The assumptions can be motivated by observation that model parameters are constant for several days.

Often persistence varies with season and hence an expected persistence for a given month can also be of interest in applications. The time variable persistence can be computed as follows

$$T(t) = \mathbb{P}(W(t) > w) / \mu(w; t) = 2\pi \sqrt{\frac{\lambda_{000}(t)}{\lambda_{002}(t)}} \Phi\left(\frac{m(t) - w^{0.6}}{\lambda_{000}(t)}\right) e^{\frac{(u^a - m(t))^2}{2\lambda_{000}(t)}}. \quad (17)$$

For the location $\lambda_{000}(t) = \sigma_f^2 + \sigma_{sl}^2 = 0.9$ while

$$\lambda_{002}(t) = \exp(-4.01 - 0.158 \cos(\omega_y t) + 0.224 \sin(\omega_y t)) + \exp(-7.92).$$

In Figure 12, left plot, $\mu(w)$ computed from model by means of (16), is compared with estimates of $\mu(w)$ derived using ERA Interim data (dashed dotted line) and in situ measurements (dotted line). The wind speeds were measured every hour giving three time denser coverage of the wind speed variability. The denser sampling affects the observed numbers of upcrossings and hence the estimated $\mu(w)$ for in situ measurements were about twice as large as $\mu(w)$ estimated for ERA Interim data. Hence we have resampled the data to achieve the same sampling intervals for the two data sets. After resampling the theoretical $\mu(u)$ agrees very well with the estimated $\mu(u)$ except for wind speeds below 5 m/ for which the approximation is less good. We conclude that the model describes well crossings of the measured winds speeds at the location.

In the right plot in Figure 12 the expected persistence computed using model is compared with the persistences estimated in ERA Interim data and from the measured wind speeds. As in the left plot, also here the solid lines show results based on theoretical model, dashed dotted lines are estimates using ERA Interim data while dotted lines estimates based on measured wind speeds. In the figure we compare persistence statistics for three levels w , 10, 15 and 20 m/s. That why there are three solid, dashed dotted and dotted lines in the right plot. Since expected persistence is decreasing function of w the highest line corresponds to persistence for $w = 10$ m/s while the lowest to the persistence for $w = 20$ m/s, for each type of lines. In the figure we have chosen to present persistence as the function of month and hence the solid lines represents $T(t)$ evaluated using (17). The remaining lines are estimates of T . We conclude that expected persistence computed using the model agrees well with the estimates.

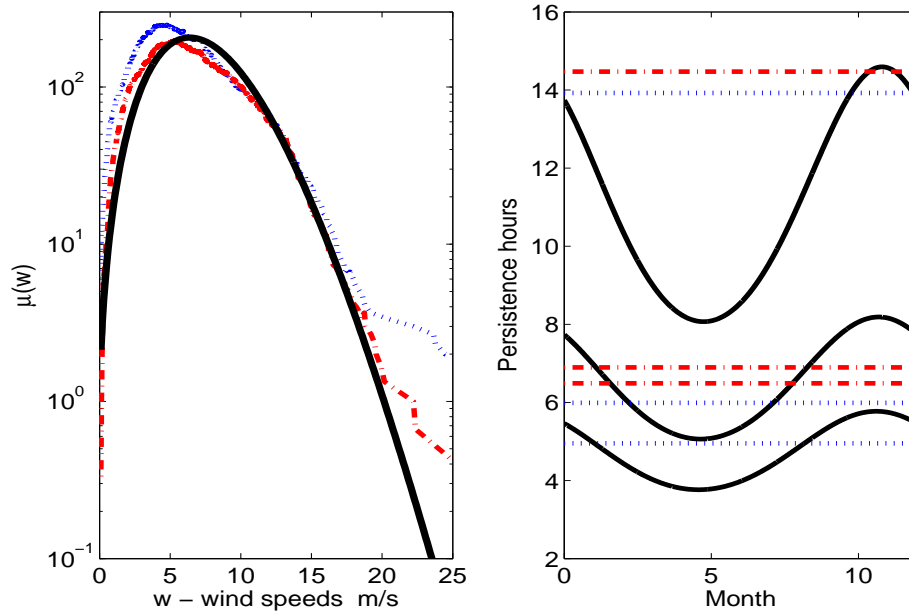


Figure 12: Left plot - Expected number of w -upcrossings $\mu(w)$, defined in (16), during one year (solid line) compared with estimates of $\mu(w)$ using ERA Interim data years 2007-2009 (dashed-dotted line) and from measured wind speeds in years 2005, 2006, 2008 (dotted line). Right plots - Solid lines present $T(t)$, defined in (17), for levels $w = 10, 15, 20$ m/s. (The persistence is a decreasing function of w .) Dotted lines are estimates of T using measured wind speeds years 2005, 2006 and 2008. Dashed dotted lines are estimates of T using ERA Interim data for years 2007, 2008 and 2009.

5 Conclusions

A simple statistical model for the wind speed field variability in time and over large geographical region has been proposed. Simple physical interpretations of model's parameters are given. The model was fitted to ERA Interim reanalyzed data. Validation tests show very good match between the distributions estimated from the data and the theoretical one computed from the model.

6 Acknowledgments

Support of Chalmers Energy Area of Advance is acknowledge. First author research was also supported by Swedish Research Council Grant 340-2012-6004 and by Knut and Alice Wallenberg stiftelse.

References

- [1] J.M. Azais, and C. Delmas. Asymptotic expansions for the distribution of the maximum of Gaussian random fields. *Extremes*, 5:181–212, 2002.
- [2] A. Baxevani and I. Rychlik. Maxima for Gaussian seas. *Ocean Engineering*, 33:895–911, 2006.
- [3] A. Baxevani, S. Caires, and I. Rychlik. Spatio-temporal statistical modelling of significant wave height. *Environmetrics*, 20:14–31, 2008.
- [4] A. Baxevani, K. Podgórski, and I. Rychlik. Velocities for moving random surfaces. *Prob. Eng. Mechanics*, 18:251–271, 2003.
- [5] A. Baxevani, K. Podgórski, and I. Rychlik. Dynamically evolving Gaussian spatial fields. *Extremes*, 14:223-251, 2011.

- [6] B.G. Brown, R.W. Katz and A.H. Murphy Time Series Models to Simulate and Forecast Wind Speed and Wind Power. *Journal of Climate and Applied Meteorology*,23:1184-1195, 1984.
- [7] D.R. Cox and V.S. Isham. A simple spatial-temporal model of rainfall. *Proc. R. Soc. Lond. Ser. A, Math. Phys. Eng. Sci.*, 415:317–328, 1988.
- [8] V.K. Gupta and E. Waymire. On Taylor’s hypothesis and dissipation in rainfall. *J. Geophys. Res.*, 92:9657–9660, 1987.
- [9] M. S. Longuet-Higgins. The statistical analysis of a random, moving surface. *Phil. Trans. Roy. Soc. A*, 249:321–387, 1957.
- [10] V. Monbet, P. Ailliot and M. Prevosto. Survey of stochastic models for wind and sea state time series. *Prob. Eng. Mechanics*, 22:113–126, 2007.
- [11] K. Podgórski, and I. Rychlik. A spatial-temporal model of significant wave height fields with application to reliability and damage assessment of a ship. *Journal of Marine systems*, 2013, doi:10.1016/j.jmarsys.2013.03.006.
- [12] S. O. Rice. The mathematical analysis of random noise part I and II. *Bell Syst Tech J.*, 23:282–332, 1944, 24:46–156, 1945.